

An Efficient Hybrid Model in Analyzing Nonlinearly Loaded Dipole Antenna above Lossy Ground in the Frequency Domain

S. R. Ostadzadeh

Department of Engineering
University of Arak, Arak, Iran
s-ostadzadeh@araku.ac.ir

Abstract — In this paper, a hybrid model is proposed for including lossy ground effect on scattering response from nonlinearly loaded dipole antenna. In this model, at first the input admittance and induced current at dipole antenna situated over lossy ground are efficiently modeled based on the fuzzy inference concepts. Volterra series model is then applied to compute the induced voltage across nonlinear load at different frequency harmonics. Numerical examples show not only the accuracy of the proposed hybrid model but also a high computational efficiency in comparison with previous hybrid models.

Index Terms — Dipole antenna, fuzzy inference, lossy ground, and nonlinear load.

I. INTRODUCTION

Nonlinear loads are connected to antennas terminal so as to protect devices against strong-strength exciting waves. A typical nonlinearly loaded antenna vertically suited above ground plane as well as its microwave equivalent circuit is shown in Fig. 1. In Fig. 1 (b), Y_{in} is the input admittance of the dipole antenna and I_{sc} is the short circuit current due to incidence of exciting waves. There are several methods for analyzing such structures in frequency domain [1-7] and time domain [8-11]. Time-domain-based analyses lead to accurate results; however, they are both relatively time-demanding, and they cannot be easily used to include the effect of lossy ground. Analysis in frequency domain on the other hand is based on solving microwave circuit in Fig. 1 (b), so that the numerical method of moments [12], MoM, for computing Y_{in} and I_{sc} , and methods of analyzing nonlinear microwave circuits [13] for

computing induced voltage across nonlinear load are combined. It is well known that these hybrid models, suffer from repetitive and time consuming computations due to changing parameters of exciting waves and lossy ground.

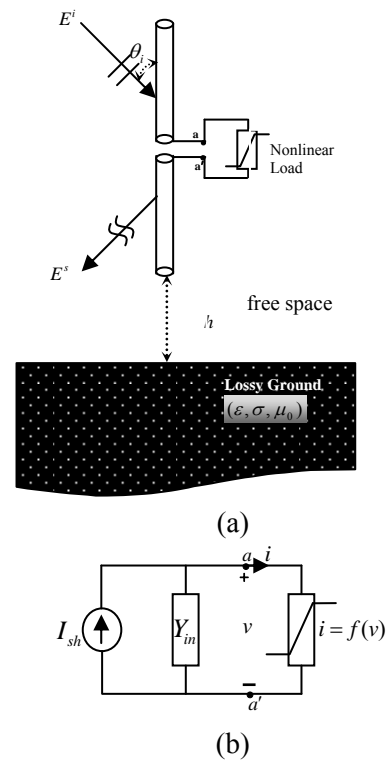


Fig. 1. (a) Schematic diagram of nonlinearly loaded dipole antenna over lossy ground and (b) microwave equivalent circuit.

Up to the author's knowledge, there is no comprehensive closed form solution for including lossy ground effect on wire antennas except in [14], restricted to $h > 0.25\lambda_0 / \sqrt{|\epsilon_r|}$ where ϵ_r is

relative complex dielectric constant of ground and in [15], which is valid for $\epsilon_r > 10$.

In order to overcome these mentioned drawbacks and restrictions, the novel model based on fuzzy inference introduced by Tayarani et al. [16] can be taken into considerations. In the previous study [17], the behavior of the dipole antenna in free space was considered as simple membership functions as shown in Fig. 2, and using that Y_{in} and I_{sc} were well predicted in free space. However, analysis of this problem in the presence of lossy ground was not addressed.

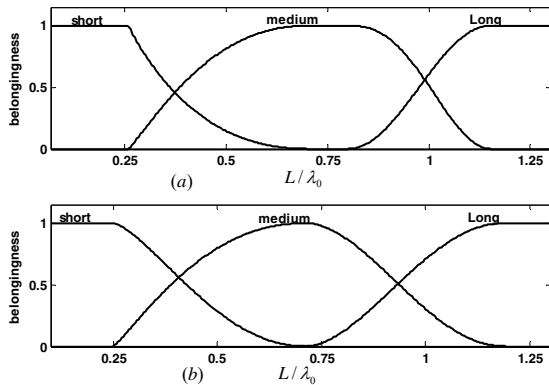


Fig. 2. The membership functions representing the behavior of the dipole antenna in free space, for (a) modeling circular movement and (b) modeling partial phase.

In this paper, at first using approximating the behavior of the dipole antenna in the presence of lossy ground with the one in free space, the effect of lossy ground on Y_{in} and I_{sc} are then easily extracted as very simple curves, and hence complete models of Y_{in} and I_{sc} in the presence of lossy ground are achieved. Volterra series model [6] is finally applied to Fig. 1 (b), so that the induced voltage at different frequency harmonics is computed.

In section II, formulation of the intelligent method [16] is briefly explained. Modeling Y_{in} and I_{sc} based on this model is given in section III. Substituting these methods in microwave equivalent circuit of Fig. 1 (b) and solving it by Volterra series is in section IV. Finally, conclusion is given in section V.

II. FORMULATION OF FUZZY MODEL

Instruction of the fuzzy-based model according to [16], for a problem is briefly explained as below:

1. Plot amplitude versus phase of output in polar plane to observe circular movement, and then find basic circles making this movement.
2. Choose three-point sets as starting points on each basic circle and then fit a circle and line on each three-point set as fuzzy inputs.
3. Define membership function for each fitted circle. These functions have belongingness one on each fitted circle and smoothly decreasing to zero on the neighbor fitted circles by the following equation,

$$\alpha(v) = \begin{cases} \frac{1}{2} (1 + \cos\pi \frac{v-a_1}{a_2-a_1})^{\beta_1} & v: a_1 \rightarrow a_2 \\ \frac{1}{2} (1 - \cos\pi \frac{v-a_1}{a_2-a_1})^{\beta_2} & v: a_1 \rightarrow a_2 \end{cases} \quad (1)$$

where β_1 and β_2 represents optimizations parameters and v is input value. Also a_1 and a_2 are points where fitted circles are completely fitted on the circular movement.

4. Infer a circle for each input value using the following inference equation,

$$\begin{cases} x(v) = \sum_{i=1}^n x_i \alpha_i(v) \\ y(v) = \sum_{i=1}^n y_i \alpha_i(v) \\ r(v) = \sum_{i=1}^n r_i \alpha_i(v) \end{cases} \quad (2)$$

in which $x_i, y_i, r_i, i = 1, 2, \dots, n$ are center coordinates and radius of the fitted circles, respectively and $x, y,$ and r as fuzzy outputs are center coordinates and radius of inferred circles for each input value. Also α_i is a membership function obtained in the previous step.

5. Fit lines on the three-point sets and infer a line for each input value to model partial phase (as defined in [16]) the same as circular movement.
6. Compute center coordinates and radius of the fitted circles for a few values of parameter, and then fit simple curves on

them to estimate the characteristics of fitted circles and lines for new values of parameter. These simple curves denote the effect of this parameter lonely on output.

- Repeat the above steps for the other parameters.

III. MODEL OF DIPOLE ANTENNA BASED ON QUALITATIVE CONCEPTS

A. Modeling input admittance

Consider a dipole antenna of length 20 cm vertically situated above a lossy ground. The ground effect is characterized by three parameters, i.e., relative dielectric constant ϵ_r , conductivity σ and vertical spacing h .

To extract the effect of the ground dielectric constant lonely, it is assumed the other ground parameters is constant ($\sigma = 0$ and $h = 0.01$ m). Hence, the amplitude versus phase of the input admittance in the frequency interval of 0.1 GHz – 2.3 GHz is shown in Fig. 3.

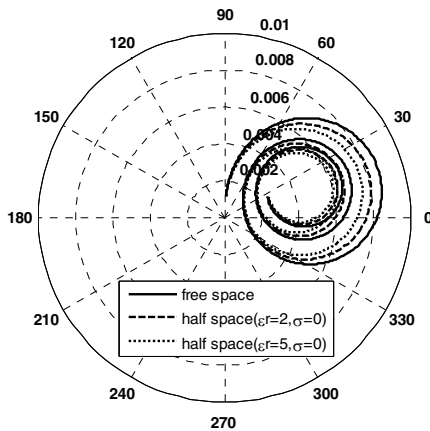


Fig. 3. The amplitude versus phase of input admittance (S) of dipole over ground for different values of ϵ_r .

As it is seen in Fig. 3, circular movements including three basic circles for different values of ϵ_r are observed. It seems that the only difference among them is center coordinates and radius of basic circles.

Therefore, at the beginning of modeling, the behaviour of the problem over lossless ground is approximated with the one in free space (Fig. 2), and then center coordinates (x_i, y_i) and radius (r_i) of fitted circles for a few values of ϵ_r are computed by

MoM and simple curves are finally fitted on them as shown in Fig. 4.

Mean while in order to show the effect of the ground with respect to free space, they are normalized to individual ones in free space denoted by (X_n, Y_n) and R_n .

Now using these simple curves as fuzzy inputs and the problem behaviour (Fig. 2), the input admittance (actual output) for each new value of relative dielectric constant is predicted. Figure 5 shows the input admittance for $\epsilon_r = 2.5$.

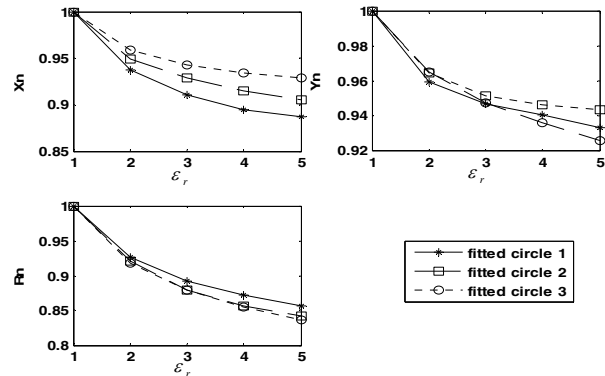


Fig. 4. The effect of the dielectric constant of ground on the input admittance using simple curves.

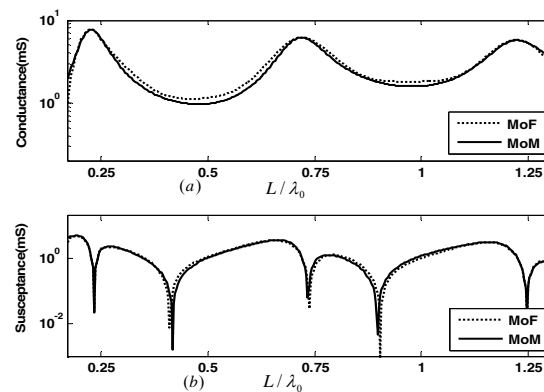


Fig. 5. The input admittance (mS) of dipole antenna suited 0.01 m away from lossless ground ($\epsilon_r = 2.5, \sigma = 0$), for (a) conductance (mS) and (b) susceptance (mS).

As it is seen, comparing the results of method of fuzzy (MoF) with accurate ones (MoM) shows excellent agreement while the run-time is considerably reduced. To include the conductivity effect of the ground on the input

admittance lonely, it is assumed that $\epsilon_r = 1$, $h = 0.01$ m, and the amplitude versus phase of the input admittance for a few values of conductivity is plotted in Fig. 6. Extracting the conductivity effect on input admittance is the same as the dielectric constant and shown in Fig. 7. Once more, using the achieved simple curves as fuzzy inputs and the behavior of the problem, the input admittance of dipole over lossy ground for each new value of conductivity is easily predicted. Meanwhile in Fig. 7, σ_n is normalized conductivity in decibel ($\sigma_n = 10\log(\sigma/0.0001)$).

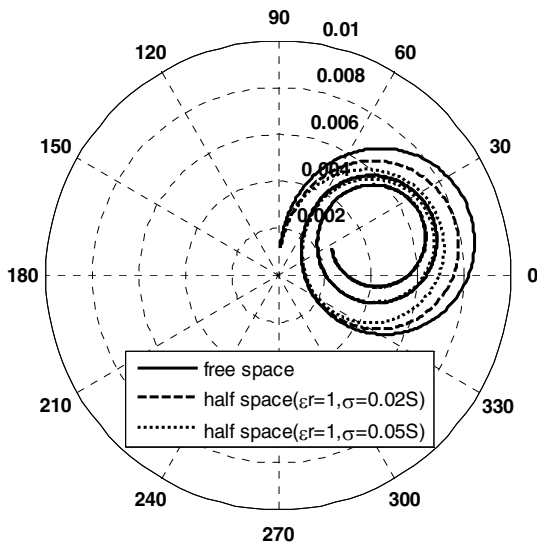


Fig. 6. The amplitude versus phase of the input admittance (S) over ground for different conductivity values.

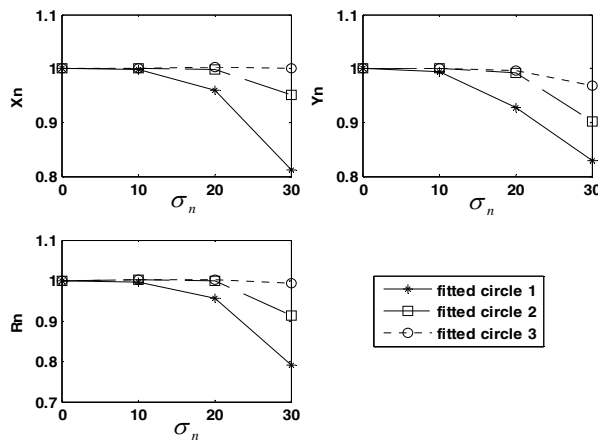


Fig. 7. The effect of conductivity on the input admittance.

In a similar manner, the effect of vertical spacing can be extracted from Fig. 8 under assuming $\epsilon_r = 1$, $\sigma = 0.0001$ (S/m), and h as a varying parameter. According to [18], spatial membership functions can be used to combine the effects of more than two parameters but they cannot be viewed as a figure. Thus, in this paper without loss of generality, the two effects of ϵ_r and σ are combined as follows,

$$\alpha_i(\epsilon_r, \sigma_n) = \begin{cases} \frac{1}{2} \left(1 - \cos \pi \left[\frac{\varphi - \varphi_2}{\varphi_1 - \varphi_2} \right]^{\beta_1} \right) & \text{for } \varphi: \varphi_1 \rightarrow \varphi_2 \quad (3) \\ \frac{1}{2} \left(1 + \cos \pi \left[\frac{\varphi - \varphi_2}{\varphi_1 - \varphi_2} \right]^{\beta_2} \right) & \text{for } \varphi: \varphi_1 \rightarrow \varphi_2 \end{cases}$$

in which

$$\varphi = \tan^{-1} \left(\frac{\epsilon_r}{\sigma_n} \right), \quad \beta_1, \beta_2 = \text{optimizing parameters}$$

and $i = \epsilon_r, \sigma_n$.

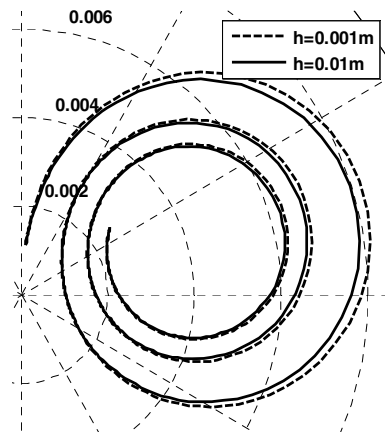


Fig. 8. The amplitude versus phase of the input admittance (S) over ground for different spacings under assuming $\epsilon_r = 1$ and $\sigma = 0.0001$ (S/m).

The spatial membership functions in this case are shown in Fig. 9. In this figure, two fuzzy sets for the two independent parameters (ϵ_r, σ_n) are seen in which each one has belongingness value of one at its individual axis and it is smoothly decreasing to zero at the other axis.

The following inferred equations can be used to extract the fitted circles versus simultaneous effects of ϵ_r and σ_n ,

$$x_j(\epsilon_r, \sigma_n) = \frac{x_j(\epsilon_r)\alpha_{\epsilon_r}(\epsilon_r, \sigma_n) + x_j(\sigma_n)\alpha_{\sigma_n}(\epsilon_r, \sigma_n)}{\alpha_{\epsilon_r}(\epsilon_r, \sigma_n) + \alpha_{\sigma_n}(\epsilon_r, \sigma_n)}$$

$$y_j(\epsilon_r, \sigma_n) = \frac{y_j(\epsilon_r)\alpha_{\epsilon_r}(\epsilon_r, \sigma_n) + y_j(\sigma_n)\alpha_{\sigma_n}(\epsilon_r, \sigma_n)}{\alpha_{\epsilon_r}(\epsilon_r, \sigma_n) + \alpha_{\sigma_n}(\epsilon_r, \sigma_n)} \quad (4)$$

$$r_j(\epsilon_r, \sigma_n) = \frac{r_j(\epsilon_r)\alpha_{\epsilon_r}(\epsilon_r, \sigma_n) + r_j(\sigma_n)\alpha_{\sigma_n}(\epsilon_r, \sigma_n)}{\alpha_{\epsilon_r}(\epsilon_r, \sigma_n) + \alpha_{\sigma_n}(\epsilon_r, \sigma_n)}$$

where $x_j(i)$, $y_j(i)$, $r_j(i)$, $i = \epsilon_r, \sigma_n$, $j = 1, 2, 3$ are center coordinates and radii of fitted circles extracted in Figs. 3 and 5. Also, α_{ϵ_r} and α_{σ_n} are spatial membership functions in Fig. 9. Finally, $x_j(\epsilon_r, \sigma_n)$, $y_j(\epsilon_r, \sigma_n)$, $r_j(\epsilon_r, \sigma_n)$ are the inferred coordinates and radii of fitted circles, respectively representing simultaneous effects of the two parameters on the input admittance as shown in Fig. 10.

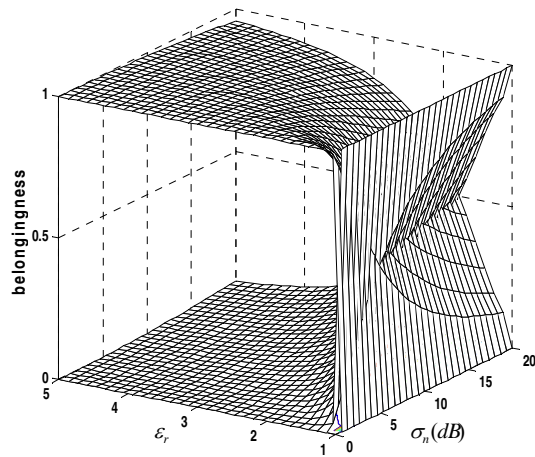


Fig. 9. Spatial membership functions for combining effects of ϵ_r and σ_n .

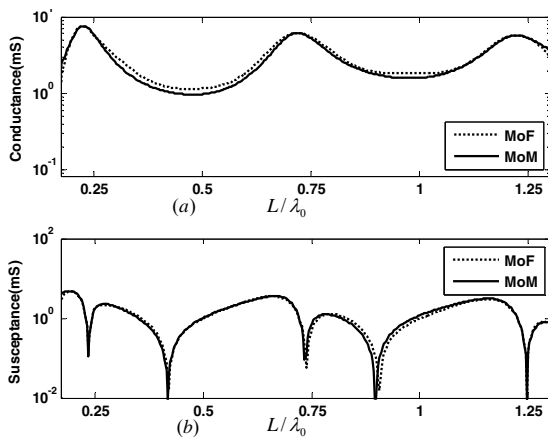


Fig. 10. The input admittance (mS) of dipole antenna suited 0.01 m away from lossy ground ($\sigma = 0.01$ S/m, $\epsilon_r = 2.5$) for (a) conductance and (b) susceptance.

From now on, using these inferred spatial fuzzy inputs and the behavior of dipole antenna in free space (Fig. 2), the input admittance of the dipole antenna over lossy ground for each value of ϵ_r , σ , and h is efficiently predicted.

B. Modeling induced current

Modeling the induced current is the same as the input admittance, thus the dielectric constant effect is only extracted. Figure 11 shows the amplitude versus phase of the induced current on the dipole antenna over lossless ground illuminated by a plane wave with incident angle $\theta_i = 50^\circ$.

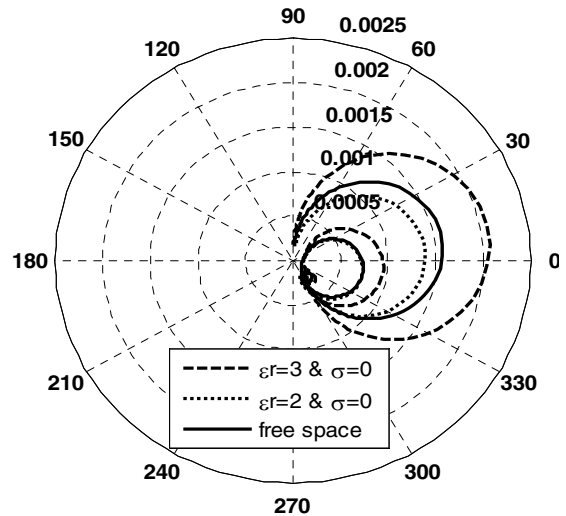


Fig. 11. The amplitude versus phase of induced current (A) for different values of dielectric constant.

In this figure, the circular movements for the induced current are observed. Hence, again approximating the behaviour of the dipole antenna over lossy ground with the one in free space (Fig. 2), the dielectric constant effect on the induced current can be easily extracted as shown in Fig. 12.

The created fuzzy system is run for $\epsilon_r = 2.5$ and $\epsilon_r = 10$. The predicted results (MoF) in addition to the accurate ones (MoM) are shown in Figs. 13 and 14, respectively. As it is seen in Fig. 13, good agreement is achieved while runtime is vanishingly short, but Fig. 14 shows considerable error between the two methods around $L/\lambda_0 = 0.45$.

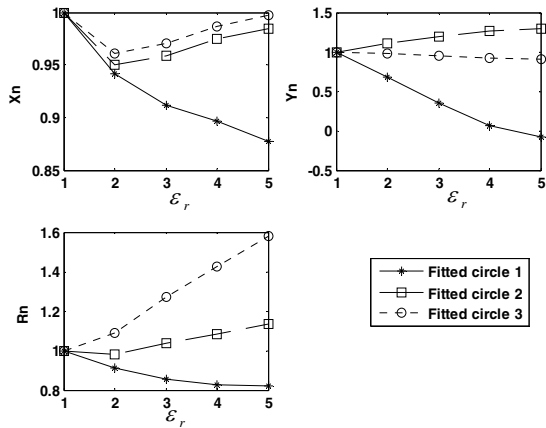


Fig. 12. Extracted relative dielectric constant effect on the induced current.

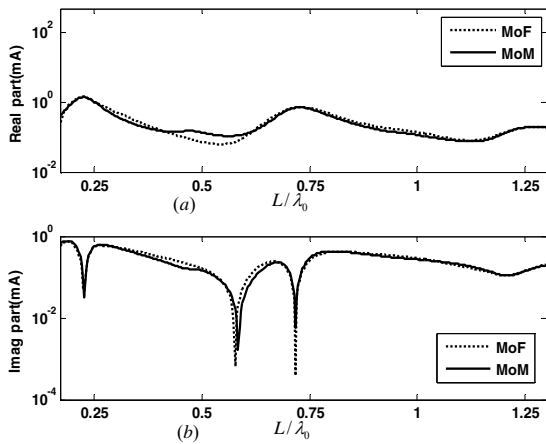


Fig. 13. The induced current computed by MoF and MoM for $\epsilon_r = 2.5$ for (a) real part (mA) and (b) imaginary part (mA).

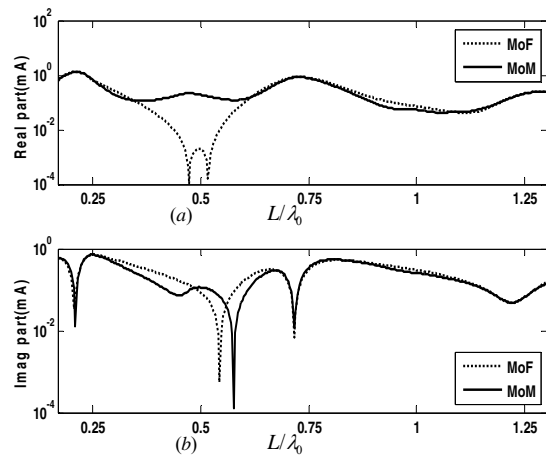


Fig. 14. The induced current computed by MoF and MoM for $\epsilon_r = 10$ for (a) real part (mA) and (b) imaginary part (mA).

To know what happens around $L/\lambda_0 = 0.45$, look exactly at the Fig. 15 showing the amplitude versus phase of the induced current for $\epsilon_r = 5$ and $\epsilon_r = 10$. According to Fig. 15, increasing relative dielectric constant, a new circle between the first and second circles is getting formed. It means that in order to predict exactly the induced current around $L/\lambda_0 = 0.45$, a fitted circle and line around $L/\lambda_0 = 0.45$ should be added (in equations (2) and (3)). Hence, according to step (3), the new membership functions for modeling circular movement and partial phase are considered and shown in Fig. 16. These new membership functions represent the behavior of the problem for high dielectric constants.

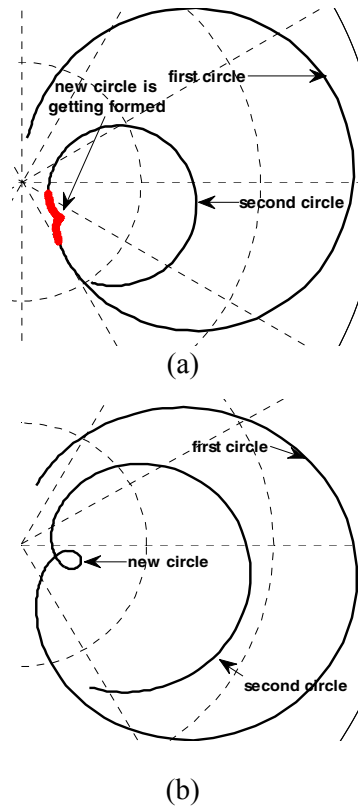


Fig. 15. The amplitude versus phase of the induced current in polar plane for, (a) $\epsilon_r = 5$ and (b) $\epsilon_r = 10$ (to distinguish circles better, the third basic circle is not shown).

Comparing Fig. 16 with Fig. 2 shows a new membership function around $L/\lambda_0 = 0.45$

representing presence of a new circle and line in this region. Now, with the use of these new membership functions, and four fitted circles and line as fuzzy inputs, the induced current for $\epsilon_r = 10$ is well predicted as shown in Fig. 17. Similar to Fig. 12, center coordinates and radius of the new fitted circle for high dielectric constants can be extracted as shown in Fig. 18.

IV. COMPUTING INDUCED VOLTAGE ACROSS NONLINEAR LOAD

Consider a dipole antenna illuminated by a plane wave with amplitude $E_i = 1$ V/m, incident angle $\theta_i = 50^\circ$ and suited 0.01 m away from a lossy ground ($\epsilon_r = 10, \sigma_n = 10dB$). This antenna is centrally loaded to a nonlinear conductance with following ($i-v$) characteristic,

$$i = \frac{1}{75}v + 4v^3 \quad (5)$$

Now substituting the predicted outputs (MoF), i.e., Y_{in} and I_{sh} , in Fig. 1 (b), and applying Volterra series [6] to it, the induced voltage across nonlinear load at frequency harmonics is computed. Figure 19 shows the induced voltage at different harmonics by two hybrid approaches.

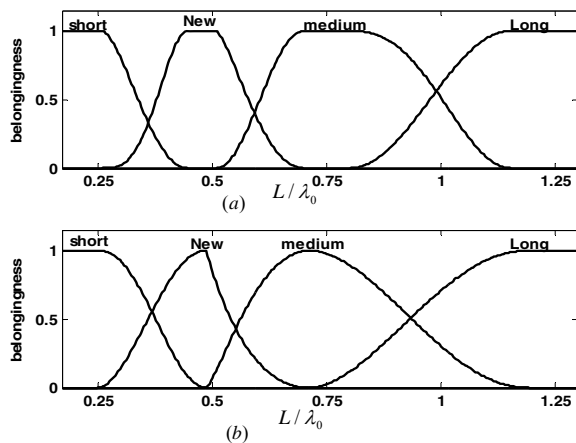


Fig. 16. The membership functions representing the problem behavior for $\epsilon_r > 5$, for (a) modeling circular movement and (b) modeling partial phase.

Table I compares the run-times of the two hybrid approaches. As it is seen, the run-time by proposed hybrid approach is considerably reduced. Meanwhile, the run-times by the proposed model

in Table I is valid after the effect of ground parameters by MoF is extracted.

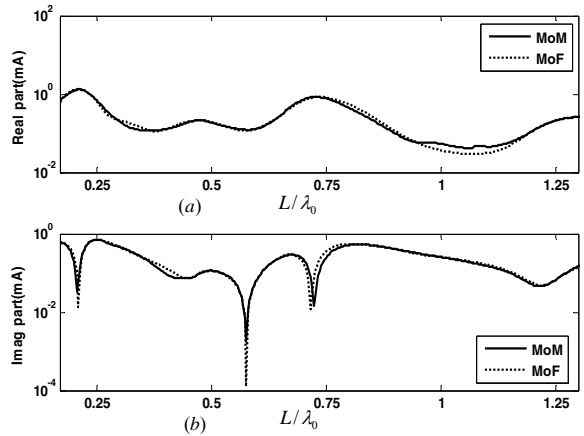


Fig. 17. The predicted induced current (mA) for $\epsilon_r = 10$ by new membership functions for (a) real part (mA) and (b) imaginary part(mA).

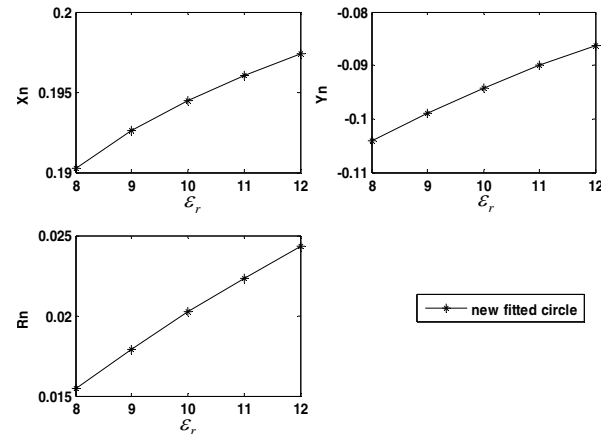


Fig. 18. Center coordinates and radius of the new fitted circle versus ϵ_r .

Table I. Comparing run-times of the two hybrid approaches for computing the induced voltage at different frequency harmonics.

Method	MoF +	MoM +
Structure	Volterra	Volterra
Problem in free space	≈ 0.3sec	≈ 34sec
Problem over ground	≈ 0.45sec	≈ 5.4 min

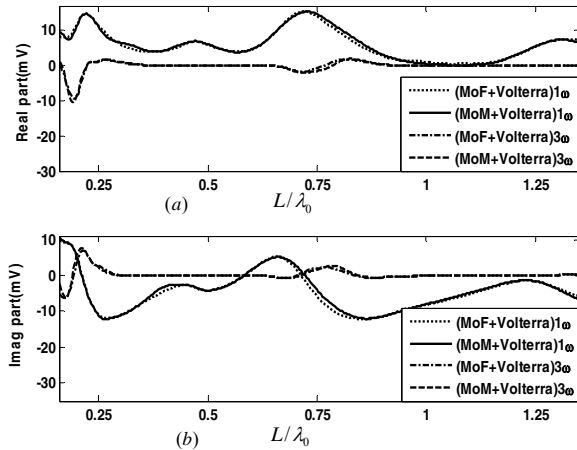


Fig. 19. Computed induced voltage (mV) at different harmonies by the two hybrid approaches for (a) real part (mV) and (b) imaginary part (mV).

V. CONCLUSION

In this paper, a combined MoF-Volterra model was proposed for analysis of nonlinearly loaded dipole antenna above imperfect ground so as to remove complex and repetitive computations. In this method, the input admittance and the induced current of the dipole antenna based upon the fuzzy inference approach was separately predicted and Volterra series was then used to compute the induced voltage at different harmonies. As a result, an efficient hybrid model is achieved. Analyzing nonlinearly loaded dipole array including mutual coupling effects is another study that can be carried out similarly.

REFERENCES

- [1] C. Huang and T. Chu, "Analysis of wire scatterers with nonlinear or time-harmonic loads in the frequency domain," *IEEE Trans. Antennas Propagat.*, vol. 41, pp. 25-30, 1993.
- [2] K. Lee, "Two efficient algorithms for the analyses of a nonlinearly loaded antenna and antenna array in the frequency domain," *IEEE Trans. Electromag. Compat.*, vol. 45, pp. 339-346, 2000.
- [3] K. Lee, "Genetic algorithm based analyses of nonlinearly loaded antenna arrays including mutual coupling," *IEEE Trans. Antennas Propagat.*, vol. 51, pp. 776-781, 2003.
- [4] K. Lee, "Mutual coupling mechanisms within arrays of nonlinear antennas," *IEEE Trans. Electromag. Compat.*, vol. 47, pp. 963-970, 2005.
- [5] K. Lee, "Application of neural networks and its extension of derivative to scattering from a nonlinearly loaded antenna," *IEEE Trans. Antennas Propagat.*, vol. 55, pp. 1126-1132, 2007.
- [6] T. Sarkar and D. Weiner, "Analysis of nonlinearly loaded multiport antenna structures over an imperfect ground plane using the Volterra-series method," *IEEE Trans. Electromag. Compat.*, vol. 20, pp. 278-287, 1978.
- [7] K. Sheshyekani, S. Sadeghi, and R. Moini, "A combined MoM-AOM approach for frequency domain analysis of nonlinearly loaded antennas in the presence of a lossy ground," *IEEE Trans. Antennas Propagat.*, vol. 56, pp. 1717-1724, 2008.
- [8] H. Schuman, "Time-domain scattering from a nonlinearly loaded wire," *IEEE Trans. Antennas Propag.*, vol. 22, no. 4, pp. 611-613, July 1974.
- [9] J. Landt, "Network loading of thin-wire antennas and scatterers in the time domain," *Radio Sci.*, vol. 16, pp. 1241-1247, Nov. 1981.
- [10] M. F. Pantoja, et al, "Transient analysis of thin-wire antennas over Debye media," *Applied Computational Electromagnetic Society (ACES) Journal*, vol. 27, no. 3, March 2012.
- [11] H. R. Karami, et al, "Transient response of nonlinearly loaded antennas above a lossy dielectric half-space: A modified AOM approach," *IEEE Trans. Electromag. Compat.*, vol. 20, pp. 1-9, March 2012.
- [12] R. Harrington, *Field Computation by Moment Methods*, Macmillan, New York, 1968.
- [13] S. Mass, *Nonlinear Microwave Circuits*, Artech House, Norwood, MA, 1988.
- [14] T. Sarkar and B. Strait, "Analysis of arbitrarily oriented thin wire antenna arrays over imperfect ground planes," *Syracuse University, Syracuse, NY, Contract F19628-73-C-0047, Tech. Report TR-75-15*, 1975.
- [15] P. Barnes and F. Tesche, "On the direct calculation of a transient plane wave reflected from a finitely conducting half-space," *IEEE Transaction on Electromag. Comp.*, vol. 33, pp. 90-96, 1991.
- [16] M. Tayarani and Y. Kami, "A qualitative analysis in engineering electromagnetics; an application to general transmission lines," *IEICE Trans. Elect.*, vol. E83-C, pp. 85-97, 2001.
- [17] S. Ostadzadeh, M. Tayarani, and M. Soleimani, "A hybrid model in analyzing nonlinearly loaded dipole antenna and finite antenna array in the frequency domain," *International Journal of RF and Microwave*, vol. 19, pp. 512-518, 2009.
- [18] S. Shouraki and N. Honda, "Outlines of a soft computer for brain simulation," *5th International Conference on Soft Computing and Information / Intelligent Systems*, pp. 545-550, 1998.